NEW CRITERIA FOR THE EDUCTION OF THREE-DIMENSIONAL TURBULENT STRUCTURES

Lionel Larchevêque
IUSTI, UMR CNRS 6595, Université de Provence (Aix-Marseille I)
5 rue Enrico Fermi, F-13453 Marseille cedex 13, France
lionel.larcheveque@polytech.univ-mrs.fr

Michèle Larchevêque
Institut Jean le Rond d'Alembert, UMR CNRS 7190, Université Pierre et Marie Curie (Paris VI)
4 place Jussieu, boîte 162, F-75252 Paris cedex 5, France
larchevq@lmm.jussieu.fr

ABSTRACT

A new family of criteria built on geometrical considerations to educe coherent structures in turbulent flow is proposed and validated using analytic and DNS three-dimensional flowfields. The ability of these criteria to educe regions of specific dynamical behavior is also demonstrated.

INTRODUCTION

In the recent years a large number of methods have been proposed to educe vortical structures with application to the visualization and the study of turbulent coherent structures. Among these methods the Q criterion by Hunt *et al.* (1988), the λ_2 criterion by Jeong and Hussain (1995) and to a lesser extent the Δ criterion by Chong *et al.* (1990) are the most popular. It is worth noting that most of methods, although resulting in distinct definitions of a vortex core for three-dimensional flowfields, boil down for incompressible two-dimensional flows to the single Weiss (1991) criterion. On the contrary, the two-dimensional criterion defined by Herbert *et al.* (1996), based on the curvature of isovorticity lines, yields more precise dynamical results and educes much thinner structures. Note nonetheless that the same geometrical considerations applied to streamlines rather than isovorticity lines results in the Weiss criterion.

The purpose of the present work is to extend the former two-dimensional definition of Herbert *et al.* (1996) to three-dimensional flows.

MATHEMATICAL FORMULATION

Local analysis of the isosurface properties

The basic idea of this section is to define an educing method based on the geometrical properties of some isosurfaces of a carefully selected quantity. It is therefore implicitly assumed that these properties are induced by the local dynamics of the flow. Only a single scalar quantity is considered and the resulting educing scheme does not rely on any arbitrary threshold so as to be "objective".

The structure of interest are generally the ones associated with high levels of the selected quantity, although it is obvious that derivations similar to the ones described hereafter could be applied to structure of low levels. For turbulent flows, the more natural choice, in the first step, is to seek for structures of high vorticity.

At each location $\mathrm{M_0}$ in the flow the local second order approximation $\mathrm{S_{M_0}}$ of the isovorticity surface associated with $\mathrm{M_0}$ is considered. Consequently the surface $\mathrm{S_{M_0}}$ is implicitly defined by:

$$\begin{aligned} \|\underline{\omega}\|_{|\mathrm{M}} - \|\underline{\omega}\|_{|\mathrm{M_0}} &= \underline{\mathrm{MM_0}} \cdot \underline{\nabla}\Big(\|\underline{\omega}\|_{|\mathrm{M_0}}\Big) \\ &+ \frac{1}{2}\,\underline{\mathrm{MM_0}}^{\mathrm{T}}\,\underline{\underline{\mathrm{H}}}(\|\underline{\omega}\|)_{|\mathrm{M_0}}\,\underline{\mathrm{MM_0}} \\ &= 0 \end{aligned} \tag{1}$$

The Hessian matrix $\underline{\underline{\mathrm{H}}}(\|\underline{\omega}\|)$ of the vorticity norm $\omega = \|\underline{\omega}\|$ is defined by

$$H_{ij}(\omega) = \frac{\partial^2 \omega}{\partial x_i\,\partial x_j} \tag{2}$$

Since $\underline{\underline{\mathrm{H}(\omega)}}$ is symmetric, its eigenvalues $\lambda_1 \leq \lambda_2 \leq \lambda_3$ are purely real and the associated eigenvectors $\left(\underline{e_1}, \underline{e_2}, \underline{e_3}\right)$ form an orthogonal basis. Thus the local behavior up to the second order is fully determined by $\left(\lambda_i, \underline{e_i}\right)_{i=1,2,3}$ and a set of three scalars a, b, c related to the projection of the gradient of ω on the basis $\left(\underline{e_1}, \underline{e_2}, \underline{e_3}\right)$:

$$\underline{\nabla}(\omega)_{|\mathrm{M_0}} = a\,\underline{e_1} + b\underline{e_2} + c\,\underline{e_3} \tag{3}$$

Equation 1 can then be rewritten in the local Euclidean frame $\left(\mathrm{M_0}, \underline{e_1}, \underline{e_2}, \underline{e_3}\right)$ as:

$$a\,X + b\,Y + c\,Z + \frac{1}{2}\left(\lambda_1\,X^2 + \lambda_2\,Y^2 + \lambda_3\,Z^2\right) = 0 \tag{4}$$

with $\underline{\mathrm{MM_0}} = X\,\underline{e_1} + Y\,\underline{e_2} + Z\,\underline{e_3}$. Eventually, when $\lambda_1\,\lambda_2\,\lambda_3 \neq 0$, Eq. 4 can be equivalently recast in:

$$\lambda_1\,\left(X + \frac{a}{\lambda_1}\right)^2 + \lambda_2\,\left(Y + \frac{b}{\lambda_2}\right)^2 + \lambda_3\,\left(Z + \frac{c}{\lambda_3}\right)^2 = K \tag{5}$$

with K defined by:

$$K = \frac{a^2}{\lambda_1} + \frac{b^2}{\lambda_2} + \frac{c^2}{\lambda_3} \tag{6}$$

The surface $\mathrm{S_{M_0}}$ is a quadric of principal axes $\left(\underline{e_1}, \underline{e_2}, \underline{e_3}\right)$ and the location of its center C is given by:

$$\underline{\mathrm{M_0C}} = -\frac{a}{\lambda_1}\,\underline{e_1} - \frac{b}{\lambda_2}\,\underline{e_2} - \frac{c}{\lambda_3}\,\underline{e_3} \tag{7}$$

Note that K can be rewritten using Eq. 7 as:

$$K = -\underline{\mathrm{M_0C}} \cdot \underline{\nabla}(\omega)_{|\mathrm{M_0}} \tag{8}$$

The positive orientation for S_{M_0} is set accordingly to $\underline{\nabla}(\omega)$, ensuring that at least one of the principal curvatures at location M_0 is positive when S_{M_0} is close to a maximum. Using this convention, the mean curvature $\mathcal{H}$ of S_{M_0} at location M_0, defined as the half-sum of the two principal curvatures $\kappa_1(M_0)$ and $\kappa_2(M_0)$, reads:

$$\mathcal{H} = \frac{-a^2\ (\lambda_2 + \lambda_3) - b^2\ (\lambda_1 + \lambda_3) - c^2\ (\lambda_1 + \lambda_2)}{2\ (a^2 + b^2 + c^2)^{\frac{3}{2}}} \qquad (9)$$

Equation 9 can be rewritten in a frame-independent form that does not require the explicit computation of the eigenvalues:

$$\mathcal{H} = \frac{\underline{\nabla}(\omega)^{\mathrm{T}}_{|M_0}\ \underline{\underline{H}}(\omega)_{|M_0}\ \underline{\nabla}(\omega)_{|M_0} - \mathrm{Tr}\Big(\underline{\underline{H}}(\omega)_{|M_0}\Big)\ \Big\|\underline{\nabla}(\omega)_{|M_0}\Big\|^2}{2\ \Big\|\underline{\nabla}(\omega)_{|M_0}\Big\|^3} \qquad (10)$$

Similarly, information contained in the eigenvalues can be recovered by considering the three main invariants of the Hessian matrix:

$$I_1 \quad = \quad \lambda_1 + \lambda_2 + \lambda_3 \quad = \quad \mathrm{Tr}\Big(\underline{\underline{H}}(\omega)_{|M_0}\Big) \qquad (11)$$

$$\begin{aligned} I_2 \quad &= \quad \lambda_1\,\lambda_2 + \lambda_1\,\lambda_3 + \lambda_2\,\lambda_3 \\ &= \quad \frac{1}{2}\left\{\left[\mathrm{Tr}\Big(\underline{\underline{H}}(\omega)_{|M_0}\Big)\right]^2 - \mathrm{Tr}\Big(\underline{\underline{H}}(\omega)_{|M_0}{}^2\Big)\right\} \end{aligned} \qquad (12)$$

$$I_3 \quad = \quad \lambda_1\,\lambda_2\,\lambda_3 \ = \ \det\Big(\underline{\underline{H}}(\omega)_{|M_0}\Big) \qquad (13)$$

Noteworthily, some analytical properties can be derived from the sign of the invariants:

$$I_2 \geq 0 \quad \Rightarrow \quad \mathcal{H} \geq 0 \qquad (14)$$

$$I_1 < 0 \quad \Rightarrow \quad \underline{\omega}.\underline{\nabla}^2(\underline{\omega}) < 0 \qquad (15)$$

Structure definitions

The eigenvalues λ_i or, equivalently, the invariants I_i can be used to build a geometrical classification among structures. For instance, the isosurface of ω can be approximated by an ellipsoid in the vicinity of locations where three negative eigenvalues are encountered. Consequently regions exhibiting three negative eigenvalues are associated with pancake-shaped vortical structures. This condition can be recast using the three main invariants, resulting in the definition of the H^p_ω criterion designed to educe pancake according to the following constraints:

$$H^p_\omega: \qquad I_1 < 0 \qquad I_2 > 0 \qquad I_3 < 0 \qquad (16)$$

Note that beyond geometrical considerations, regions educed using the H^p_ω criterion are also associated with a local maximum of ω.

Next the Burgers vortex and Burgers vortex layer are analyzed in order to refine the study of the invariants on a physical basis. These two analytical flowfields are solutions of the three-dimensional incompressible Navier–Stokes equations that correspond to an equilibrium between a Gaussian vortex and a transverse straining field. The vorticity field is one-dimensional and its norm reads:

$$\omega_{\mathrm{BV}} \quad = \quad \frac{\alpha\Gamma}{4\pi\nu}\exp\left[-\frac{\alpha\left(x_1^2 + x_2^2\right)}{4\nu}\right] \qquad (17)$$

$$\omega_{\mathrm{BVS}} \quad = \quad \frac{\Gamma}{\sqrt{2\pi}}\sqrt{\frac{\alpha}{\nu}}\exp\left(-\frac{\alpha\,x_2^2}{2\nu}\right) \qquad (18)$$

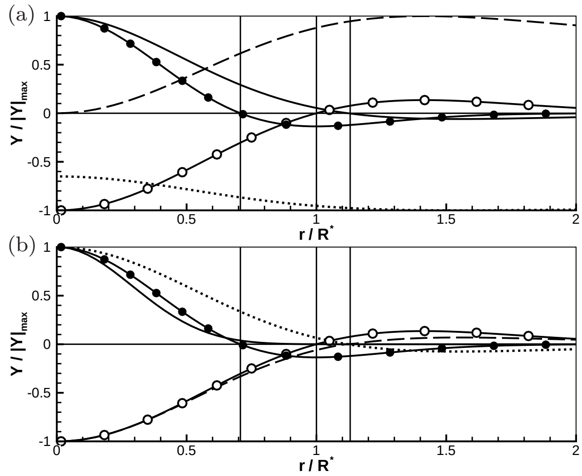

Figure 1: Profiles of Δ (———), Q (– – –), λ_2 (······), $I_1^{\mathbf{H}(\omega)}$ (—○—) and $I_2^{\mathbf{H}(\omega)}$ (—●—) for Burgers' vortices with (a) $\mathrm{Re}_\Gamma = 1$ and (b) $\mathrm{Re}_\Gamma = 100$.

respectively for Burgers' vortex and vortex layer, with Γ being the total circulation, α being the parameter controlling the strain and ν being the kinematic viscosity.

By enforcing $I_1 < 0$, the classical definition of the vorticity core radius $r^* = 2\sqrt{\nu/\alpha}$ of the Burgers vortex is recovered whatever the $\mathrm{Re}_\Gamma = \Gamma/(4\pi\nu)$ is, as seen in Fig. 1. It implies that I_1 is insensitive to the transverse strain, as well as I_2, (again see Fig. 1) while I_3 is identically equal to zero. The Δ criterion also shares this property although the radius of the region educed by this criterion is slightly larger than r^*, the cancellation point of Δ corresponding to the maximal radial velocity. On the contrary Q and λ_2 criteria educe vortices only for values of Re_Γ respectively higher than $\sqrt{3}$ and 1. The radii of the educed region rise jointly with the value of Re_Γ and the same radius as for the Δ criterion is recovered within the limit $\mathrm{Re}_\Gamma \to \infty$.

The $I_1 < 0$ constraint also yields the eduction of the Burgers vortex layer with the expected thickness $\delta = \sqrt{\alpha/\nu}$. The difference with the others criteria is in this case more striking since Δ, Q and λ_2 lead to the exclusion of the whole sheet. Nonetheless, it is worth noting that Burgers' vortex layer does not meet constraints of Eq. 16 associated with the H^p_ω criterion for pancake eduction since both I_2 and I_3 are uniformly equal to zero for this flowfield.

The change in the sign of I_1 resulting in the correct definition of the characteristic lengths for both Burgers' flowfields, it is therefore assumed that $I_1 < 0$ is a necessary condition in the present definition of a vortical structure.

Apart of the pancake shape, vortical structures can be mainly classified into tubes or sheets. Such structures can be modeled in space as hyperboloids corresponding to one positive and two negative eigenvalues. In the invariant space, this condition reads $(I_1 < 0, I_3 \geq 0)$.

The discrimination between tubes and sheet is carried out on the basis of their slenderness by means of the I_2 invariant: a positive value of I_2 ensures that the hyperbolic positive eigenvalue is low enough compared with the two elliptic negative ones according to the inequality:

$$I_2 > 0 \quad \Leftrightarrow \quad \lambda_3 < \frac{\lambda_1\,\lambda_2}{|\lambda_1 + \lambda_2|} \qquad (19)$$

Geometrically speaking, such a condition on I_2 results in a slender hyperboloid. The H^t_ω criterion designed for educing

Table 1: Definitions of the members of the $\mathrm{H}_\omega^{\mathrm{xx}}$ family according to the sign of the invariants of $\underline{\underline{\mathrm{H}}}(\omega)$, Q and the mean curvature of the isovorticity surface $\mathcal{H}$.

	$\mathrm{H}_\omega^{\mathrm{p}}$	$\mathrm{H}_\omega^{\mathrm{t}}$	$\mathrm{H}_\omega^{\mathrm{rs}Q}$	$\mathrm{H}_\omega^{\mathrm{ps}Q}$	$\mathrm{H}_\omega^{\mathrm{rs}\mathcal{H}}$	$\mathrm{H}_\omega^{\mathrm{ps}\mathcal{H}}$
I_1	< 0	< 0	< 0	< 0	< 0	< 0
I_2	> 0	> 0	≤ 0	≤ 0	≤ 0	≤ 0
I_3	< 0	≥ 0	≥ 0	≥ 0	≥ 0	≥ 0
Q			> 0	≤ 0		
$\mathcal{H}$					> 0	≤ 0

tubular vortices is therefore defined as:

$$\mathrm{H}_\omega^{\mathrm{t}}: \qquad I_1 < 0 \qquad I_2 > 0 \qquad I_3 \geq 0 \tag{20}$$

Note that for Burgers' vortex the $\mathrm{H}_\omega^{\mathrm{t}}$ criterion educes a smaller region that the one corresponding to the single condition $I_1 < 0$ since the cancellation radius of I_2 is $r_0 = r^* / \sqrt{2}$. This location also corresponds to the inflexion point of the ω profile. Regarding the Burgers vortex layer, the $\mathrm{H}_\omega^{\mathrm{t}}$ criterion excludes it entirely since $I_2 = 0$ for that flow.

Complementary to tubes, sheets are educed in regions where the following constraints are met:

$$I_1 < 0 \qquad I_2 \leq 0 \qquad I_3 \geq 0 \tag{21}$$

Another subdivision between layers located close to a vortex core and plane sheets is nonetheless desirable since it is generally acknowledged that these two kinds of layers have distinct dynamical behaviors. Such a splitting appears to be difficult to obtain if based solely on the three invariants of $\underline{\underline{\mathrm{H}}}(\omega)$. It can nonetheless be achieved by taking into account other considerations.

It has been seen previously that the Q criterion excludes the whole Burgers vortex layer while it educes Burgers' vortex at least for sufficiently high Reynolds numbers. Therefore rotational / plane sheets could be discriminated by seeking for positive / negative values of Q. The criteria standing for the rotational and plane sheets by taking into account both the constraints of Eq. 21 and the Q splitting are hereafter referred to as $\mathrm{H}_\omega^{\mathrm{rs}Q}$ and $\mathrm{H}_\omega^{\mathrm{ps}Q}$.

Such a splitting may have a direct physical significance since negative values of Q are associated with regions where the strain rate dominates the rotation rate and therefore presumably regions exhibiting rather high local levels of kinetic energy dissipation. Consequently the plane sheets educed by $\mathrm{H}_\omega^{\mathrm{ps}Q}$ may match the dissipative sheets surrounding vortex cores highlighted by some authors (see for instance Horiuti, 2001). However one may note that this splitting is intrinsically specific to the study of vortical structures, regardless of other scalar quantities. Moreover $\mathrm{H}_\omega^{\mathrm{rs}Q}$ and $\mathrm{H}_\omega^{\mathrm{ps}Q}$ criteria are no longer Re_Γ-independent when applied to Burgers' vortex because of the Q dependency on the transverse strain.

Another splitting, more general and fully independent of Re_Γ, can be obtained by considering the mean curvature $\mathcal{H}$. For the Burgers vortex, Eq. 21 yields the eduction of the region $r^* / \sqrt{2} < r < r^*$ surrounding the core. The mean curvature $\mathcal{H} = (2\,r)^{-1}$ is strictly positive over this region while it is equal to zero when considering the Burgers vortex layer. Consequently, rotational / plane sheets are respectively associated with strictly positive / negative value of $\mathcal{H}$. Coupling this condition with Eq. 21 leads to the definition of the $\mathrm{H}_\omega^{\mathrm{rs}\mathcal{H}}$ and $\mathrm{H}_\omega^{\mathrm{ps}\mathcal{H}}$ criteria.

By taking into account these refinements related to vortical sheets, the whole family of the $\mathrm{H}_\omega^{\mathrm{xx}}$ criteria can be summed up according to Tab. 1. Note that the implicitly defined criterion resulting in the eduction of the regions matching the union of all the regions educed by any of the $\mathrm{H}_\omega^{\mathrm{xx}}$ criteria will be referred to as H_ω.

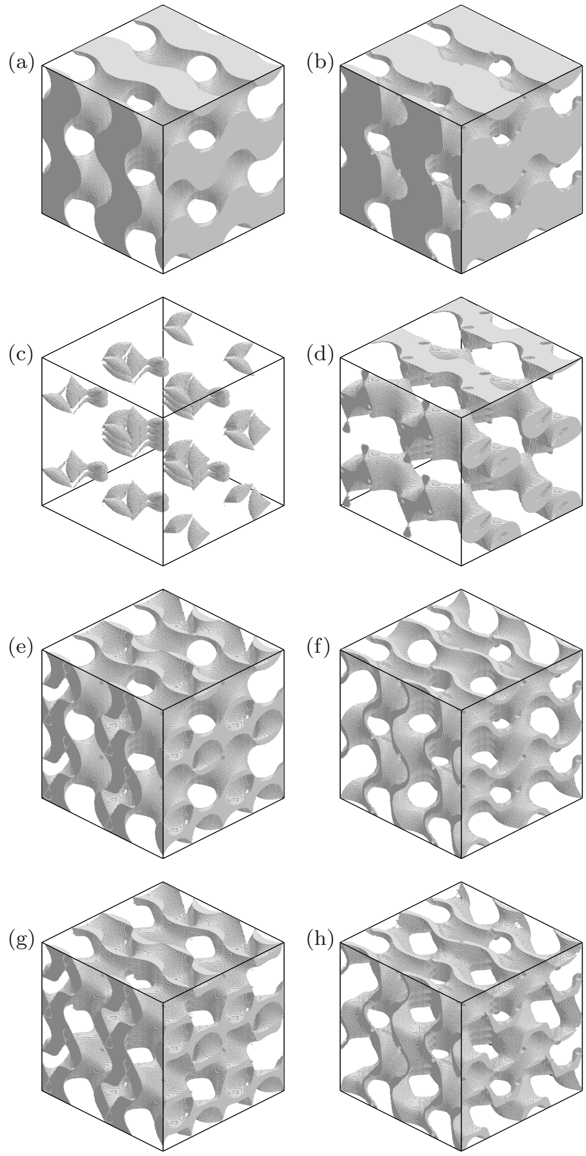

Figure 2: Structures educed from the ABC flow defined in Eq. 22 using various criteria: (a) Q, (b) H_ω, (c) $\mathrm{H}_\omega^{\mathrm{p}}$, (d) $\mathrm{H}_\omega^{\mathrm{t}}$, (e) $\mathrm{H}_\omega^{\mathrm{rs}Q}$, (f) $\mathrm{H}_\omega^{\mathrm{ps}Q}$, (g) $\mathrm{H}_\omega^{\mathrm{rs}\mathcal{H}}$ and (h) $\mathrm{H}_\omega^{\mathrm{ps}\mathcal{H}}$.

TEST CASES

ABC flow

The ABC flowfields are 2π-periodic solutions of the three-dimensional Euler equations defined by :

$$\left\{\begin{array}{lcl} u_1 & = & A\sin(x_3) + C\cos(x_2) \\ u_2 & = & B\sin(x_1) + A\cos(x_3) \\ u_3 & = & C\sin(x_2) + B\cos(x_1) \end{array}\right. \tag{22}$$

with $A = \sqrt{3}$, $B = \sqrt{2}$ and $C = 1$ resulting in chaotic streamlines. The analysis of such a flowfield in term of vortex dynamics is rather meaningless because of the equality between velocity and vorticity fields. However it is useful to check the ability of the H_ω^{xx} criteria to discriminate between structures on a geometrical basis.

The regions educed by the Q and H_ω criteria are plotted in Fig. 2 (a) and (b). Is is seen from these plots that the H_ω criterion yields a slightly larger educed region than Q but with the same global shaping. The region related to the various subdivisions of the H_ω are plotted in Fig. 2 (c) to (h). The expected geometrical shapes are recovered for both $\mathrm{H}_\omega^{\mathrm{p}}$ (Fig. 2 c) and $\mathrm{H}_\omega^{\mathrm{t}}$ (Fig. 2 d) criteria. Figures 2 (e) to (h) demonstrate that the use of I_2 to discriminate between tubes and vortex layers effectively results in educing layers located around the tubes. Lastly it is seen from Figs. 2 (e-f) and (g-h) that the separation between rotational layers and plane sheets either based on Q or $\mathcal{H}$ leads to similar educed region with sheets located outside of rotational layers.

Direct numerical simulation

Isotropic turbulence. Two instantaneous fields coming from DNS computations with a spectral resolution of 256^3 are used in this section to analyze the flow dynamics by conditional averaging over regions educed using various criteria. The first snapshot is related to a $\mathrm{Re}_\lambda \simeq 150$ computation of forced isotropic turbulence by Vincent and Meneguzzi (1991) and the second one corresponds to a freely decaying turbulence with $\mathrm{Re}_\lambda \simeq 50$, coming from computations by Liechtenstein *et al.* (2005).

Quantities analyzed are the educed volume, the turbulent kinetic energy and its dissipation rate, the enstrophy, the budget terms of the enstrophy equation and the ratio $\langle\Omega^2\rangle/\langle S^2\rangle$. Results for H_ω, Δ, Q and λ_2 regions are displayed in Tab. 2 both as a percentage of the total mean quantities and as a "density" (quantity contains in the educed volume divided by this volume), normalized by the overall density.

The H_ω, Q and λ_2 criteria yield the eduction of a similar percentage of the total volume over which there is no noticeable variation in the turbulent kinetic energy density compared to the overall value, as seen in the first three lines of Tab. 2. On the contrary, H_ω results in educing regions with a dissipation rate above the average and well above the ones seen on Q, λ_2 or even Δ regions. Such a behavior could be related to the highlighting of the small scales by the H_ω criterion that results from the wavenumber scaling of $\underline{\underline{\mathrm{H}}}(\omega)$ invariants in concordance with a power of the third derivative of the velocity field. As a matter of fact, it can be checked by computing spectra of the quantities involved in the definition of the criteria that both Q and λ_2 variables yield similar spectra whose high wavenumber relative fraction is lower that the one of Δ spectrum and far lower than the ones found for I_1, I_2 and I_3 spectra.

Focusing on the enstrophy, it is found that all criteria, as expected, educe regions of high levels compared to the average one. However the dynamics of the enstrophy, revealed by analyzing the terms of its transport equation, differs noticeably from one educed region to another. The H_ω regions exhibit a high level of "production" related to the vortex stretching, a low level of dissipation, a high level for the sum of dissipation and diffusion and consequently a very high level of diffusion while the other criteria overall educe regions of rather large production, average dissipation and high diffusion. It is worth noting that the large density for the sum of the diffusion and dissipation of enstrophy found in H_ω regions is a consequence of relation 15 which states that this sum is negative everywhere in regions where $I1 < 0$.

Table 2: Percentage of the total value and density normalized by the mean density in regions educed using the H_ω, Δ, Q and λ_2 criteria for isotropic turbulence, either freely decaying with $\mathrm{Re}_\lambda \simeq 50$ or forced with $\mathrm{Re}_\lambda \simeq 150$. The quantities studied are respectively the volume V, the turbulent kinetic energy $k = \frac{1}{2}\langle u_i\, u_i\rangle$, the dissipation rate of k, $\epsilon = \nu\,\langle S_{ij}\, S_{ij}\rangle$, the enstrophy $\langle\omega^2\rangle = \langle\Omega_{ij}\,\Omega_{ij}\rangle$, the "production" rate of enstrophy $\mathrm{P}(\omega^2)= \langle\omega_i\,\omega_j\, S_{ij}\rangle$, the dissipation rate of enstrophy $\mathrm{d}(\omega^2)= \nu\langle\omega_{i,j}\,\omega_{i,j}\rangle$, the sum of dissipation and diffusion rates of enstrophy $\mathrm{D}(\omega^2)= \nu\langle\omega_i\,\omega_{i,jj}\rangle$, the vortex stretching rate $\mathrm{V.S.R.} = \langle\omega_i\,\omega_j\, S_{ij}\,/\,(\omega_i\,\omega_i)\rangle$and the ratio between the main rotation and strain rates $\langle\Omega_{ij}\Omega_{ij}\rangle/\langle S_{ij}S_{ij}\rangle$ with $S_{ij} = 0.5\,(\partial u_i/\partial x_j + \partial u_j/\partial x_i)$ and $\Omega_{ij} = 0.5\,(\partial u_i/\partial x_j - \partial u_j/\partial x_i)$. The operator $\langle\cdot\rangle$ denotes a conditional averaging over the educed volumes.

	H_ω	Δ	Q	λ_2
V	42–44%	62–70%	39–42%	39–43%
k	41–43% 096–0.98	62–70% 0.98–0.99	39–41% 0.96–0.98	38–42% 0.97–0.99
ϵ	48–49% 1.09–1.18	52–62% 0.83–0.89	31–34% 0.75–0.82	29–35% 0.72–0.81
ω^2	63–69% 1.51–1.55	85–87% 1.24–1.36	69–72% 1.66–1.82	69–70% 1.61–1.78
$\mathrm{P}(\omega^2)$	69–76% 1.66-1.72	73–75% 1.14–1.18	58–59% 1.42–1.49	52–53% 1.27–1.34
$\mathrm{d}(\omega^2)$	34–38% 0.82–0.85	62–71% 0.99–1.01	41–44% 1.0–1.01	39–44% 1.02–1.05
$\mathrm{D}(\omega^2)$	84–88% 1.89–2.08	79–84% 1.2–1.27	65–68% 1.56–1.65	61–66% 1.56–1.68
V. S. R.	53–56% 1.25–1.28	45–48% 0.72–0.73	29–33% 0.74–0.79	25–32% 0.63–0.75
$\langle\Omega^2\rangle/\langle S^2\rangle$	1.28–1.42	1.39–1.57	2.02–2.31	2.0–2.36

Interestingly, the study of the vortex stretching rate (penultimate line of Tab. 2) demonstrates that the high level of production in the H_ω regions is strongly induced by the vortex stretching process while in regions corresponding to the other criteria the above-average level is rather related to an preexistent high level of enstrophy. The large vortex stretching rate is also a sign that the H_ω regions are significantly involved in the turbulent cascade process.

Also note that the ratio of the conditionally averaged Ω^2 and S^2 is found to be about 1.3 in H_ω regions. Such a value is lower than for the other criteria but well above the overall average value of 1, as expected for a criterion designed to educe vortical structures.

Lastly, an indirect assessment of the coherent nature of the structures educed by means of the H_ω criterion is obtained. When applying this criterion to a coherent field resulting from a wavelet decomposition of the $\mathrm{Re}_\lambda = 150$ computation (see Roussel *et al.*, 2005, for details) and then when conditionally averaging the quantities computed from the *total* (coherent+incoherent) flowfield in the educed regions, results almost identical to those of Tab. 2 are found.

Since the H_ω regions exhibit rather different dynamics than their Δ, Q, and λ_2 counterparts, it is of interest to consider the overlapping of two regions educed using different criteria. The first line of Tab. 3 shows that more than 50 % of the H_ω educed volume are shared with volume educed by one of the other criteria. Other lines demonstrate that, when both criteria educe regions exhibiting the same trend, this one is reinforced in the intersecting regions compared

Table 3: Percentages of volume of the H_ω region also meeting another criterion and density of various quantities in the intersecting region. Results are compiled from isotropic turbulence, either freely decaying with $Re_\lambda \simeq 50$ or forced with $Re_\lambda \simeq 150$. See Tab. 2 for definitions.

	Δ	Q	λ_2
V	73–80%	54–59%	52–58%
k	0.96–0.98	0.96–0.98	0.96–0.98
ϵ	0.94–1.07	0.86–1.0	0.83–0.99
$\langle\omega^2\rangle$	1.71–1.85	2.1–2.25	2.06–2.23
$P(\omega^2)$	1.78–1.86	1.98–2.13	1.82–1.97
$d(\omega^2)$	0.89–0.90	0.96–1.0	0.94–0.98
$D(\omega^2)$	2.09–2.32	2.38–2.68	2.34–2.61
V. S. R.	1.0–1.04	0.93–0.95	0.83–0.86

Table 4: Percentage of the total value and density normalized by the mean density in regions educed using the H_ω^{p}, H_ω^{t}, $H_\omega^{rs\mathcal{H}}$ and $H_\omega^{ps\mathcal{H}}$ criteria for isotropic turbulence either freely decaying with $Re_\lambda \simeq 50$ or forced with $Re_\lambda \simeq 150$. See Tab. 2 for definitions.

	H_ω^{p}	H_ω^{t}	$H_\omega^{rs\mathcal{H}}$	$H_\omega^{ps\mathcal{H}}$
V	6–7%	11–12%	20–21%	4–5%
k	6–7% 0.95–1.0	11–12% 0.96–0.99	20–21% 0.95–0.98	4–5% 0.95–0.98
ϵ	7–8% 1.09–1.39	13–14% 1.11–1.33	21–23% 1.04–1.07	5% 1.07–1.1
ω^2	13–15% 2.17–2.23	20–23% 1.88–1.93	25–26% 1.21–1.23	5–6% 1.10–1.12
$P(\omega^2)$	16–17% 2.57-2.85	26–27% 2.25–2.34	24–27% 1.2–1.26	5–6% 1.2
$d(\omega^2)$	6% 0.90–1.05	10% 0.87–0.92	15–18% 0.77–0.84	3% 0.67–0.72
$D(\omega^2)$	20–22% 3.14–3.71	31–33% 2.5–2.9	28–29% 1.33–1.4	4–6% 1.02–1.11
V. S. R.	9% 1.37–1.51	16–17% 1.38–1.43	22–25% 1.09–1.19	5–6% 1.16–1.18
$\langle\Omega^2\rangle/\langle S^2\rangle$	1.56–2.06	1.41–1.72	1.14–1.18	1.02–1.04

to each of the individual region. When trends differ, there is globally a cancellation effect. These facts clearly demonstrate that the H_ω criterion is complementary to the family of the three other ones.

The pertinency of the H_ω criterion being established, the characteristics seen in each of the regions educed by its subcomponents have to be analyzed. The results of this analysis are displayed in Tab. 4. One has to specify that only the splitting of the vortex layer based on the mean curvature $\mathcal{H}$ ($H_\omega^{rs\mathcal{H}}$ and $H_\omega^{ps\mathcal{H}}$ criteria) has been retained. As a matter of fact the discrimination of the layer relying on Q results in difference in dynamics almost identical to those seen in the whole regions where Q is positive/negative. Their dynamics being fully driven by Q, the regions educed using the $H_\omega^{rsQ}/H_\omega^{psQ}$ criteria appear to be of little interest in the context of the present work.

The $H_\omega^{rs\mathcal{H}}$ criterion is the one yielding the eduction of the largest volume, with about twice the volume educed by the H_ω^{t} criterion and respectively three and four times the volumes educed by the H_ω^{p} and $H_\omega^{ps\mathcal{H}}$ criteria. Overall, the trends seen when analyzing the global H_ω criterion are exacerbated when going from the $H_\omega^{ps\mathcal{H}}$ criterion to the $H_\omega^{rs\mathcal{H}}$ criterion and then the H_ω^{t} and H_ω^{p} ones, with the exception of the dissipation of enstrophy for which the ordering is inverted. It therefore demonstrates that the geometrical subdivisions of the H_ω criterion is meaningful when studying the dynamics of the vortical structures.

One may nonetheless note that for the dissipation of kinetic energy and the vortex stretching rate, the dividing line is rather found between the union of pancake-shaped and tubular regions on the one hand and both kinds of vortex layer on the other hand. The roughly same level of enstrophy production is also found inside the two kinds of layers. It also seems that there is a global Reynolds number effect on both the dissipation of kinetic energy and the enstrophy densities in the four sub-regions, although the low number of analyzed flowfields prevents of affirmative conclusions.

Lastly, it is worth noting that when using one of the Δ, Q, λ_2 criteria with a threshold different to zero such as to obtain the same low volume percentage as for the H_ω^{p} criterion, density levels of dissipation of the turbulent energy, of enstrophy, of its production and of the sum of its dissipation and its diffusion are found higher in these regions than in the H_ω^{p} ones. However densities of vortex stretching rate and dissipation of enstrophy remain by far respectively lower and higher than in the H_ω^{p} regions. This fact confirms the complementarity of the both family of criteria.

Homogeneous turbulence. Two kinds of decaying homogeneous turbulent flowfields are tested complementary to the isotropic case in order to check the ability of the H_ω^{xx} criteria to educe regions with specific geometrical characteristics in real flows. The turbulence is respectively vertically stratified or in rotation around the vertical axis, as described in Liechtenstein *et al.* (2005). Note that both computations correspond to a decay time similar to the one found in the isotropic computation previously analyzed.

Due to their small-scale nature, the H_ω^{xx} criteria are not well-suited for visualization of a turbulent flow, especially for the H_ω^{t} and $H_\omega^{rs\mathcal{H}}$ ones that result in the eduction of a rather large fraction of the flow. Meaningful pictures can nonetheless be obtained be seeking for singly-connected structures and by displaying the largest ones only. Since for H_ω^{t} the largest structure is huge and visually fill the entire volume, it has been discarded. Such a trick does not work for $H_\omega^{rs\mathcal{H}}$ and therefore no plot have been dedicated to this criterion.

For isotropic turbulence, the H_ω^{p} criterion educed lines of small pancakes mainly constricted in the inner core of strong vortices, as identified by using the Q criterion with a high threshold. It therefore explains the tubular shapes seen in the left part of Fig. 3. The H_ω^{t} criterion (right part of the figure) also educes tubular regions but of less slenderness and being much more interleaved. Left parts of Figs 3 (b-c) highlight more clearly the expected pancake shape obtains for regions educed by the H_ω^{p} criterion with an orientation selected by the specific physics of the flow. Geometrical expectation are also met for the H_ω^{t} criterion.

The plots of Fig. 4 dedicated to the regions educed using the $H_\omega^{ps\mathcal{H}}$ criterion are more difficult to analyze. It can nonetheless be seen that, at least for non-isotropic flows, the sheet regions effectively exhibit flattened vortical structures, mostly surrounding pancakes or tubular regions.

Lastly, it may be noted that for the non-isotropic flows the hierarchy of structure types in term of increasing/decreasing densities is for some quantities altered in non-trivial ways compared with the one found for isotropic flows, although more flowfields are needed to trustfully confirm that point.

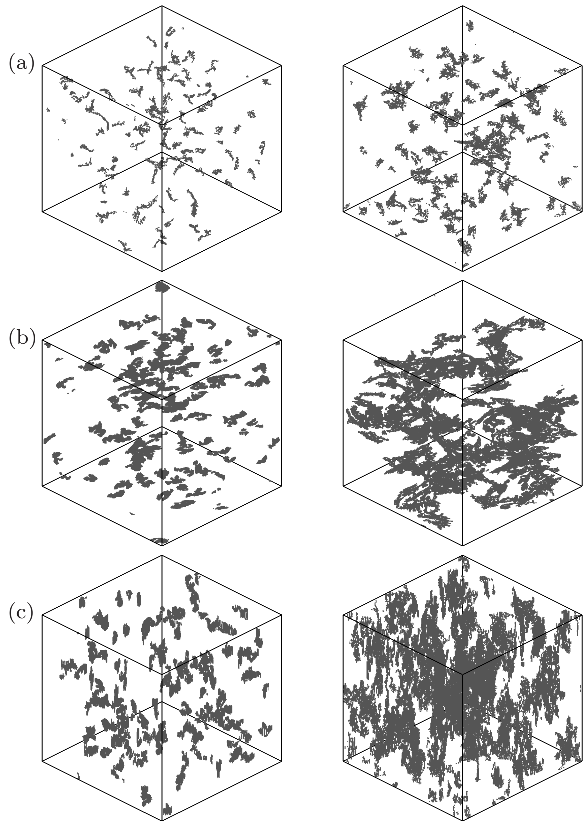

Figure 3: Visualization of the 100 largest structures educed according to the $\mathrm{H}_\omega^{\mathrm{p}}$ (left) and $\mathrm{H}_\omega^{\mathrm{t}}$ (right) criteria from freely decaying (a) isotropic, (b) stratified and (c) rotating homogeneous turbulent flowfields. Note that for the $\mathrm{H}_\omega^{\mathrm{t}}$ plots the largest structure has been discarded because of its wide spatial extension making it unsuitable for visualization.

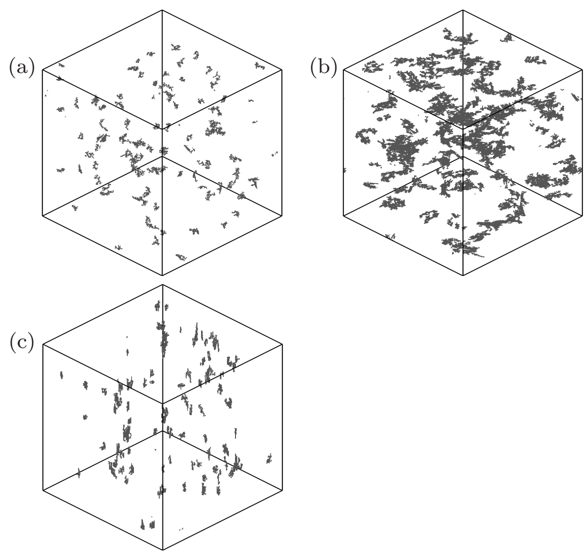

Figure 4: Visualization of the 100 largest structures educed according to the $\mathrm{H}_\omega^{\mathrm{ps}_\mathcal{H}}$ criterion from freely decaying (a) isotropic, (b) stratified and (c) rotating turbulent flowfield.

CONCLUSION

A new family of geometric criteria designed to educe turbulent structures has been defined. These criteria allow a clear splitting of vortical structures into pancakes, tubes, rotational layers and sheets when the vorticity magnitude is considered. Moreover they do not involve the use of any threshold.

The structures thus highlighted exhibit a high level of enstrophy, enstrophy production, vortex stretching rate and enstrophy diffusion but a low level of enstrophy dissipation. Therefore these structures can be seen as small-scale enstrophy sources.

Because of their small-scale nature, the $\mathrm{H}_\omega^{\mathrm{xx}}$ criteria are not well-suited for visualization of turbulent flows. However, because their definitions is free from arbitrary threshold, they could be used to objectively analyze the local temporal evolution of vortical structures and their dynamics in time-dependant flows such as decaying turbulence.

It is also worth noting that these kinematic criteria satisfy the Galilean invariance and can be applied to any scalar quantity α as long as it is Galilean invariant. They can for instance be used with $\alpha = Q$ or $\alpha = \lambda_2$ to objectively seek for strong vortical structures among the $Q\,/\,\lambda_2$ regions without using arbitrary thresholds.

No explicit knowledge of the eigenvalues of the Hessian matrix of α is required since quantities involved are tensorial invariants and can be evaluated in any Euclidean frame. However note that in the present case high-order or spectral schemes are mandatory for computing the invariants since they involved the use of second derivatives of the vorticity.

REFERENCES

Chong, M. S., Perry, A. E., and Cantwell, B. J., 1990, "A general classification of three-dimensional flow fields", *Phys. Fluids A*, Vol. 2 (5), pp. 765–777.

Herbert, V., Larchevêque, M., and Staquet, C., 1996, "Identification des structures organisées en écoulement bidimensionnel", *C. R. Acad. Sci. Paris Sér. II b*, Vol. 323 (8), pp. 519–526.

Horiuti, K., 2001, "A classification method for vortex sheet and tube structures in turbulent flows", *Phys. Fluids*, Vol. 13 (12), pp. 3756–3774.

Hunt, J. C. R., Wray, A. A., and Moin, P., 1998, "Eddies, stream, and convergence zones in turbulent flows", *Proceedings of the 1988 summer program*, CTR, Stanford, pp. 193–208.

Jeong, J., and Hussain, F., 1995, "On the identification of a vortex", *J. Fluid Mech.*, Vol. 285, pp. 69–94.

Liechtenstein, L., Godeferd, F. S., and Cambon, C., 2005, "Nonlinear formation of structures in rotating stratified turbulence", *Journal of Turbulence*, Vol. 6 (24), pp. 1–18.

Roussel, O., Schneider, K. and Farge, M., 2005, "Comparaison of orthogonal and biorthogonal wavelets for coherent structures extraction", *Journal of Turbulence*, Vol. 6 (11), pp. 1-15.

Vincent, A., and Meneguzzi, M., 1991, "The spatial structure and statistical properties of homogeneous turbulence", *J. Fluid Mech.*, Vol. 225, pp. 1–20.

Weiss, J., 1991, "The dynamics of enstrophy transfer in two-dimensional hydrodynamics", *Physica D*, Vol. 48 (2-3), pp. 273–294.